Development 118, 1063-1075 (1993)
Printed in Great Britain © The Company of Biologists Limited 1993

Loss of *Hox-A1* (*Hox-1.6*) function results in the reorganization of the murine hindbrain

Ellen M. Carpenter, Judy M. Goddard, Osamu Chisaka, Nancy R. Manley and Mario R. Capecchi*

Howard Hughes Medical Institute, Department of Human Genetics, University of Utah School of Medicine, Salt Lake City, Utah 84112, USA

*Author for correspondence

SUMMARY

Targeted disruption of the murine *hox-A1* gene results in severe defects in the formation of the hindbrain and associated cranial ganglia and nerves. Carbocyanine dye injections were used to trace afferent and efferent projections to and from the hindbrain in *hox-A1*$^{-}$/*hox-A1*$^{-}$ mutant mice. Defects were observed in the position of efferent neurons in the hindbrain and in their projection patterns. In situ hybridization was used to analyze the transcription pattern of genes expressed within specific rhombomeres. *Krox-20, int-2 (fgf-3),* and *hox-B1* all display aberrant patterns of expression in *hox-A1*$^{-}$ mutant embryos. The observed morphological and molecular defects suggest that there are changes in the formation of the hindbrain extending from rhombomere 3 through rhombomere 8 including the absence of rhombomere 5. Also, motor neurons identified by their axon projection patterns which would normally be present in the missing rhombomere appear to be respecified to or migrate into adjacent rhombomeres, suggesting a role for *hox-A1* in the specification of cell identity and/or cell migration in the hindbrain.

Key words: *Hox* genes, rhombomere, segmentation, mouse development

INTRODUCTION

The development of the vertebrate hindbrain is characterized by the transient appearance of rhombomeres, which are morphologically distinct bulges in the walls of the hindbrain. The presence of rhombomeres in all vertebrates suggests that segmental organization is an evolutionarily conserved developmental strategy to build and diversify the hindbrain. At the cellular level, it has been suggested that rhombomeres are lineage restriction units; cells arising after the appearance of boundaries between rhombomeres do not cross the established borders (Fraser et al., 1990). Further, structures within the hindbrain show a metameric organization consistent with their segmental origin. For example, the branchiomotor neurons providing efferent fibers for the Vth, VIIth, and IXth cranial nerves arise in chick rhombomeres with a 2-segment periodicity, with each motor pool respecting the boundaries between pairs of adjacent rhombomeres (Lumsden and Keynes, 1989; reviewed in Lumsden, 1990).

Segmental organization is also reflected at the molecular level. The expression patterns of a number of genes encoding presumptive transcription factors respect the boundaries between adjacent rhombomeres. By analogy with the function of homologous genes in *Drosophila*, such genes are excellent candidates for establishing the segmental pattern in the murine hindbrain and/or for specifying the identity of cells within the rhombomeric units. For example, *krox-20*, a gene encoding a zinc-finger protein, is expressed in two stripes at the level of rhombomeres 3 and 5 (Wilkinson et al., 1989a). The expression patterns of members of the *Hox* gene family also respect rhombomere boundaries (Wilkinson et al., 1989b; Murphy et al., 1989). *Hox-A1* (*hox-1.6*; in this article we are using the new *Hox* gene nomenclature proposed by Scott, 1992) has an anterior limit of expression that terminates at the boundary between rhombomeres 3 and 4. A member of the *Hox B* family, *hox-B1* (*hox-2.9*), is also initially expressed up to the prospective boundary between rhombomeres 3 and 4. Subsequently, *hox-B1* expression retreats caudally but leaves a single stripe of expression in rhombomere 4 (Wilkinson et al., 1989b; Frohman et al., 1990; Murphy and Hill, 1991).

The observations that the *Hox* genes are similar in structure and organization to the genes of the *Drosophila Homeotic* complex, and that they are differentially expressed in murine hindbrain rhombomeres, suggest that these genes play a role in rhombomere specification and/or subsequent cell fates within these segmental units (Duboule and Dollé, 1989; Graham et al., 1989). Mutation of one member of the *Hox A* family, *hox-A1*, has previously been shown to affect the morphology of the developing hindbrain, cranial nerves, and ear (Lufkin et al., 1991; Chisaka et al., 1992). Of particular interest is the observation that *hox-A1*$^{-}$/*hox-A1*$^{-}$ mice lack the characteristic repeating bulges of hindbrain rhombomeres (Chisaka et al., 1992). *Hox-A1* is expressed in mouse embryos as early as E7.5, and by E8.0

is found in the developing nervous system to an anterior limit between rhombomeres 3 and 4. Expression subsequently retreats posteriorly and by E8.5 of development, *hox-A1* is no longer expressed in the hindbrain or associated mesoderm (Murphy and Hill, 1991).

Hindbrain segmentation may play a critical role in the patterning of head development in the region affected by the disruption of *hox-A1*. In vertebrates, this region of the hindbrain provides segmental information in the form of cranial nerves, which emanate from alternate rhombomeres (Lumsden and Keynes, 1989), in the precise positioning of efferent neurons contributing to these nerves (Lumsden and Keynes, 1989) and in the partitioning of neural crest cells from alternate rhombomeres into separate branchial arches (Lumsden et al., 1991; Serbedzija et al., 1992). Disruption of this segmentation might be expected to result in rearrangement of peripheral structures as has previously been observed in *hox-A1*$^-$ mutant animals. Therefore, it was critical to determine whether *hox-A1* acts directly on the enumeration of hindbrain segmentation or whether it affects only the subsequent specification of cells within rhombomeres and the associated peripheral structures. The previous studies described only the gross morphology of the developing hindbrain and its associated ganglia, but made no attempt to elucidate the cellular or molecular changes within the mutant hindbrain.

We have examined both the cellular and molecular organization of the developing hindbrain in *hox-A1* mutant mice. To examine rhombomeric organization, we have used carbocyanine dye tracing to determine the position and projection pattern of neurons providing efferent fibers to cranial nerves V, VII/VIII, and IX in embryos homozygous for the *hox-A1*$^-$ disruption. These mice show a number of hindbrain abnormalities. Primarily, neurons contributing efferent fibers to the VIIth/VIIIth cranial nerves are radically displaced. The expression pattern of three segmentally expressed genes, *krox-20*, *int-2* (*fgf-3*) and *hox-B1*, were used as morphological markers to examine further rhombomeric organization in *hox-A1*$^-$/*hox-A1*$^-$ embryos. The changes in the position and projection patterns of the branchiomotor pool as well as in the expression patterns of *krox-20*, *int-2*, and *hox-B1* are consistent with a severe disruption of hindbrain formation. In *hox-A1*$^-$ animals this reflects a shortening of the hindbrain as well as a loss of rhombomere 5 morphological markers. Reorganization of the hindbrain is apparent from rhombomeres 3 through 8. These direct effects of the *hox-A1* mutation on hindbrain formation may underlie some of the previously observed peripheral mutant phenotypes.

MATERIALS AND METHODS

Generation of mice

Mice heterozygous for a targeted disruption of the *hox-A1* gene (containing a neomycin resistance gene inserted into the homeobox region, Chisaka et al., 1992) were intercrossed to produce embryos, some of which were homozygous for disruption of the gene. These mice were used for dye injections and for in situ hybridization experiments as described below. Mice carrying a targeted *E. coli lac-Z* insertion into the *int-2* gene (*int-2*^{lacZ}) were generated as described (Mansour et al., 1993). Expression of β-galactosidase in these mice reflected the RNA expression pattern of the *int-2* gene. Mice heterozygous for *int-2*^{lacZ} were crossed with *hox-A1*$^+$/*hox-A1*$^-$ mice to produce mice heterozygous for both the *hox-A1* deficiency and for *int-2*^{lacZ}. These parents were either intercrossed or crossed with *hox-A1*$^+$/*hox-A1*$^-$ mice to produce embryos homozygous for the *hox-A1* deficiency (*hox-A1*$^-$/*hox-A1*$^-$) and heterozygous for *int-2*^{lacZ}.

Genotype analysis

Genotypes of embryos were determined using Southern blot analysis of yolk sac DNA as previously described (Chisaka et al., 1992; Mansour et al., 1993) or using PCR. For the PCR screen, yolk sacs from each embryo were collected into PCR lysis buffer (McMahon and Bradley, 1990). DNA was amplified using 2 sets of primers. The first set consisted of a sequence 5′ to the inserted neomycin resistance gene (*hox-A1* 5′ primer) and a sequence 3′ to the homeobox in an untranslated region of the gene (*hox-A1* 3′ primer). The second set was a sequence from the 3′ end of the inserted neomycin resistance gene (Neo primer) and the *hox-A1* 3′ primer. The primer sequences were as follows: *hox-A1* 5′ primer, 5′GTGGAGATTGCCGCGTCCCTACAGCTCAAT3′; *hox-A1* 3′ primer, 5′AGGAAAGGATGTTGGGAGCCATCAGCAATT3′ (Lufkin et al., 1991); Neo primer, 5′GCCTTCTATCGCCTTCTTGACGAGTTCTTC3′ (Lufkin et al., 1991). These combinations of primers resulted in generation of 2 PCR products, one of 471 bp (from the wild-type *hox-A1* gene using the *hox-A1* 5′ and 3′ primers) and one of 504 bp (from the disrupted *hox-A1* gene using the Neo and *hox-A1* 3′ primers). The PCR reaction was carried out in a 50 μl final volume containing 50 mM KCl, 1.5 mM $MgCl_2$, 10 mM Tris (pH 8.3), 0.01% gelatin, 5% DMSO, 250 μM of each dNTP, 250 ng of each primer and 1 unit of Taq polymerase (Cetus). Temperature cycling was 94°C, 1 minute; 55°C, 1 minute; 72°C, 2 minutes plus 1 additional second per cycle repeated for 32 cycles. PCR products were separated on a 5% polyacrylamide gel and detected using ethidium bromide staining.

Dye injections

11 litters of mice were obtained from intercrosses between *hox-A1*$^+$/*hox-A1*$^-$ parents. Embryos were collected at days 11.5 through 12.5 of embryonic development (E11.5-E12.5). The day a copulation plug was observed was considered E0.5. A total of 85 embryos were examined, 20 homozygous wild-type (*hox-A1*$^+$/*hox-A1*$^+$), 47 heterozygotes (*hox-A1*$^+$/*hox-A1*$^-$), and 18 homozygous mutant (*hox-A1*$^-$/*hox-A1*$^-$) embryos. Embryos were collected from timed, pregnant females and pinned ventral side up on Sylgard-coated Petri plates. Animals were fixed for 2 hours in 4% paraformaldehyde, rinsed briefly in phosphate buffer, and dissected to expose the ventral surface of the hindbrain and the adjacent cranial ganglia. Three cranial ganglia, the trigeminal (V), the facial (VII), and the glossopharyngeal/vagal complex (IX/X) were chosen to receive injections of the fluorescent carbocyanine dyes, DiI and DiO (Molecular Probes). The dyes were prepared as a 0.25% solution in dimethylformamide and were pressure injected into the cranial ganglia or into their adjacent cranial nerves. In 67 animals from 9 litters, DiO was injected into the Vth ganglion and DiI was injected into the VIIth ganglion. Some of these animals received a second injection of DiO into the IX/X complex. In these cases, injections were aimed at the IXth ganglion or its adjacent nerve, but due to the close proximity of the Xth ganglion, cells and fibers in this ganglion were often labeled as well. 18 animals from 2 additional litters were used for analysis of the Vth ganglion efferents alone. In these animals, DiI was injected only into the Vth ganglion. The animals were left for 48 hours at room temperature for the dye to be transported and then they were mounted and viewed using fluorescein and rhodamine filter systems on a Leitz Ortholux microscope equipped with epifluorescence illumination.

DiO appears green using a fluorescein filter set, while DiI appears yellow-green with a fluorescein filter set and red with a rhodamine filter set. Animals were photographed using Kodak Ektachrome 400 or 400 HC film.

int-2^{lacZ}/hox-A1 mice

A total of 103 E9.5 embryos were obtained from thirteen litters of crosses as described above. 55 were *int-2^{+}/int-2^{lacZ}*, and of these, 16 were *int-2^{+}/int-2^{lacZ}, hox-A1^{-}/hox-A1^{-}*. Embryos were collected, fixed and reacted with X-Gal as previously described (Mansour et al., 1993). No background staining from endogenous β-galactosidase was observed. Whole animals were photographed using transillumination on a dissecting microscope. Selected animals were subsequently embedded in paraffin, sectioned (10 μm), counterstained with nuclear fast red (Mansour et al., 1993), and examined under dark-field optics on a Leitz Ortholux microscope. Under these conditions, the X-Gal product appears pink. Sections were photographed using a didymium filter and 40 M magenta viewing filter. Eleven embryos of genotype *int-2^{+}/int-2^{lacZ}, hox-A1^{-}/hox-A1^{-}* were examined in detail.

In situ hybridization

Hox-A1 homozygous mutant mice and their heterozygous and wild-type littermates were examined by in situ hybridization with probes for *krox-20* and *hox-B1*. *Krox-20* expression was examined in whole-mount in situ preparations, while *hox-B1* expression was examined in sectioned animals. Embryos used for analysis were collected from timed pregnant females at E8-E9.5. The whole-mount in situ hybridization protocol used was kindly provided by J. McMahon.

For *krox-20* whole-mount in situ hybridization, embryos were fixed in 4% paraformaldehyde overnight, then processed as described by Bally-Cuif et al. (1992). Hybridization was carried out overnight at 70°C in 50% formamide, 5× SSC (pH 5), 50 μg/ml torula RNA and 50 μg/ml heparin with the addition of 1 μg/ml digoxigenin-labeled *krox-20* probe. Embryos were washed as described (Bally-Cuif et al., 1992), treated with 100 μg/ml RNase A and 100 units/ml RNase T1 in 0.5 M NaCl, 10 mM Tris (pH 7.5), 0.1% Tween-20 at 37°C, then washed again. Embryos were incubated in 10% heat-treated sheep serum (Jackson Laboratories) in TBST (1.5 mM NaCl, 0.03 mM KCl, 0.025 M Tris pH 7.5, 0.1% Tween-20) with 2 mM levamisole for 2.5 hours, then were incubated overnight at 4°C in a 1:1000 dilution of alkaline phosphatase-conjugated anti-digoxigenin antibody (Boehringer Mannheim) in TBST with 10% sheep serum. Antibodies were diluted to 1:100 and preabsorbed against E9.5 embryo fragments prior to use. An alkaline phosphatase-mediated color reaction was carried out using 333 μg/ml 4-nitroblue tetrazolium chloride (Boehringer Mannheim) and 165 μg/ml 5-bromo-4-chloro-3-indolyl phosphate (Boehringer Mannheim). The color reactions were carried out overnight at room temperature. Color reactions were stopped by washing in PBST (0.137 M NaCl, 2.68 mM KCl, 6.48 mM Na_2HPO_4, 647 mM KH_2PO_4 with 0.1% Tween-20) containing 5 mM EDTA. Embryos were postfixed overnight in MEMFA (0.1 M MOPS, pH 7.4, 2 mM EGTA, 1 mM $MgSO_4$, and 3.7% formaldehyde; Harland, 1991), then rinsed and stored in PBST/EDTA. Embryos were photographed with Kodak 160T film using a Wild dissecting microscope equipped with a fiber optic light source. *Krox-20* RNA probes were prepared by transcription of a 535 base pair *Apa*I-*Hpa*I fragment from the 3′ untranslated region of *krox-20* cDNA beginning at nucleotide 1763 (Chavrier et al., 1988) using T3 or T7 RNA polymerase in a reaction mix containing 0.83 mM digoxigenin-11-UTP (Boehringer Mannheim). Control experiments using a sense probe resulted in no apparent signal (data not shown). 18 E8.5 whole embryos (3 *hox-A1^{+}/hox-A1^{+}*, 8 *hox-A1^{+}/hox-A1^{-}* and 7 *hox-A1^{-}/hox-A1^{-}*) and 6 E9.5 sectioned embryos (2 of each genotype) were examined for *krox-20* RNA expression.

For *hox-B1* analysis, embryos were collected and fixed overnight in 4% paraformaldehyde, embedded in paraffin, sectioned at 8 μm, and collected on polylysine-coated slides. Sections were treated with 20 μg/ml proteinase K for 7.5 minutes, acetylated, and hybridized under conditions described by Frohman et al. (1990). The probe used was a ^{35}S-labeled antisense RNA probe complementary to the DNA sequence of the *hox-B1* gene encompassing nucleotides 889-1173 (Frohman et al., 1990). This sequence is 3′ to the homeobox and includes some 3′ untranslated region, similar to probe 1 of Frohman et al. (1990). Control experiments using a sense probe resulted in no apparent signal (data not shown). Dehydrated slides were exposed to Kodak XAR-5 film for 3 days for preliminary analysis, then were dipped in Kodak NTB-2 nuclear emulsion diluted 1:1 with 0.6 M ammonium acetate and exposed for 2 weeks at 4°C. After developing, the sections were counterstained with Meyer's hematoxylin. Selected sections were photographed using Kodak 64T film with bright-field and/or dark-field optics on a Leitz Ortholux microscope. A total of 8 E9.5 embryos were examined for *hox-B1* expression (3 *hox-A1^{+}/hox-A1^{+}*, 1 *hox-A1^{+}/hox-A1^{-}*, and 4 *hox-A1^{-}/hox-A1^{-}*).

RESULTS

Position of branchiomotor neurons in the control mouse hindbrain

Previous observations on developing chick (Lumsden and Keynes, 1989) and mouse hindbrains (Marshall et al., 1992; Baker and Noden, personal communications) have demonstrated a precise and stereotypic pattern of development of the branchiomotor system (reviewed in Lumsden, 1990). Carbocyanine dye injections made into the cranial ganglia of both control and *hox-A1^{-}* homozygous mutant mouse embryos revealed highly organized patterns of sensory fiber and motor neuron labeling. Dye injections were made between E11.5 and E12.5 shortly after the disappearance of morphologically identifiable rhombomeres. However, based on observations in chick (Lumsden and Keynes, 1989) and mouse (Marshall et al., 1992;and a map provided by Baker and Noden, personal communications), we extrapolated the positions of the rhombomeres as shown in the schematic mouse hindbrain map presented in Fig. 1. Data used to generate this map resulted from examination of 54 control wild-type or heterozygous embryos in which DiO was injected into the Vth cranial ganglion, DiI was injected into the VIIth/VIIIth complex, and in some embryos DiO was injected into the IXth and/or Xth ganglion. Two representative examples of these embryos are shown in Fig. 2; A and C show each hindbrain viewed with fluorescein optics and B and D show the same hindbrain respectively, viewed with rhodamine optics. DiO (green label) is visible only under fluorescein optics, while DiI (yellow-green or red label) is visible under both conditions of illumination. Dye injection into these ganglia labeled both sensory and motor fibers entering and leaving the ganglia. Sensory afferent fibers projected to the hindbrain while the primarily motor efferent fibers projected away from the hindbrain. Motor fiber fills resulted in retrograde labeling of the hindbrain branchiomotor neurons giving rise to these fibers (Fig. 2; schematized in Fig. 1).

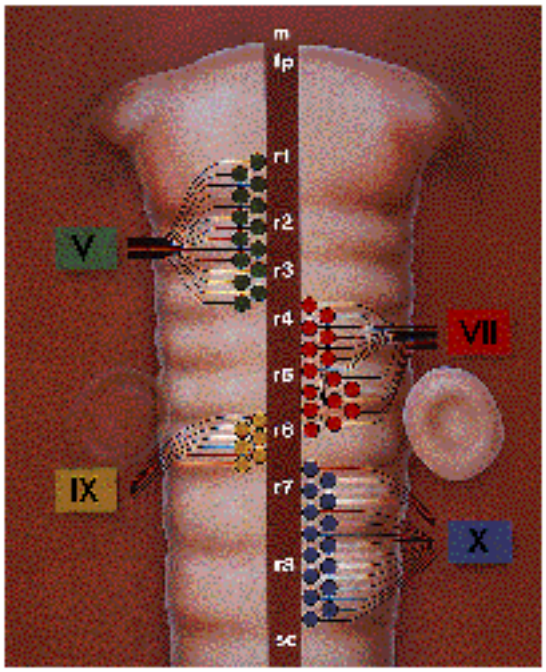

Fig. 1. Schematic representation of the position of efferent neurons in the murine hindbrain. Neurons contributing to cranial nerve V (green circles) are positioned in rhombomeres (r) 1, 2, and 3; axons from these neurons (black lines) leave the hindbrain through the lateral wall of r2. Neurons contributing to cranial nerve VII (red circles) are positioned medially in r4 and r5, as well as slightly more laterally in r5. Cranial nerve VII axons leave the hindbrain at r4. VIIIth nerve efferents also are positioned in r4 and exit the hindbrain at r4 (not shown). IXth nerve motor neurons (yellow circles) are positioned in r6 and leave the hindbrain at the same level. Xth nerve motor neurons (blue circles) are positioned medially in r7 and r8 and leave the hindbrain in several rootlets through the walls of both rhombomeres. Rhombomere boundaries are depicted by darker shading; positions of different branchiomotor neuron pools respect these boundaries. The otocyst is positioned lateral to the hindbrain at the level of r5 and r6. m fp, midline floorplate; sc, spinal cord.

Injections made into the Vth cranial ganglion in control animals filled the multiple trigeminal roots as they entered the hindbrain at the level of rhombomere 2 (see Figs 1, 2). Large bundles of afferent fibers bifurcated immediately after the point of nerve entry and travelled rostrally and caudally within the ventrolateral mantle layer (Figs 2A,C, 3A). Motor neuron cell bodies providing efferent fibers to the Vth nerve were observed more medially, positioned in rhombomeres 2 and 3, with a few cell bodies observed in rhombomere 1 (Figs 2A, 3A). Because cranial nerve V is composed of mostly afferent fibers (Altman and Bayer, 1982), the observed motor fiber population was small compared to the number of afferent fibers contributing to this nerve. Even following multiple injections, the DiO-labeled Vth ganglion branchiomotor neuron population was sometimes difficult to see. Therefore, since DiI fluoresces much more strongly than DiO under the available excitation conditions, DiI was injected into the Vth ganglia of 13 additional control embryos. In these embryos, labeled neurons were consistently observed in rhombomeres 1, 2 and 3 (Fig. 3A). Following both types of dye injection, the position of the Vth cranial nerve entering rhombomere 2 and the bifurcation of afferent fibers in the mantle layer were always visible. This label provided a landmark for the location of rhombomere 2 even in the more weakly labeled, DiO-injected embryos.

The VIIth and VIIIth cranial nerves enter the hindbrain in control animals as a single, tightly bound fascicle at the level of rhombomere 4 (Figs 1, 2). Efferent fibers entering cranial nerve VII in control mouse hindbrains arise from motor neurons positioned primarily in rhombomeres 4 and 5, with a few motor neurons located in the anterior portion of rhombomere 6. These neurons are positioned medially, adjacent to the central canal in rhombomeres 4 and 5, as well as more laterally in rhombomere 5. Motor neurons in rhombomere 4 project laterally to exit the hindbrain through the VIIth cranial nerve. Medial motor neurons in rhombomere 5 project anteriorly, then laterally, while lateral motor neurons have axons initially directed laterally, then anteriorly. Both sets of axons exit the hindbrain through rhombomere 4 (Figs 1, 2). Sensory efferent fibers contributing to the VIIIth cranial nerve also reside in rhombomere 4; axons from these cells exit the hindbrain through rhombomere 4. The populations of axons in rhombomeres 4 and 5 form a fan shape which is readily apparent when the hindbrain is viewed with rhodamine optics (Fig. 2B,D).

The IXth and Xth cranial ganglia and nerves are situated very close to each other at the posterior edges of the otocysts. The IXth cranial nerve enters the hindbrain in a single fascicle at the level of rhombomere 6 (Figs 1, 2C). Motor pools contributing efferent fibers to this nerve are positioned in rhombomere 6 and sometimes overlap with the posterior motor neurons contributing fibers to the VIIth nerve. The Xth nerve normally exits the hindbrain as a series of multiple rootlets at the levels of rhombomeres 7 and 8 (Figs 1, 2C). Motor neurons contributing to the Xth nerve are found in rhombomeres 7, 8 and more posteriorly in the spinal cord (Fig. 1).

Reorganization of hindbrain motor nuclei in *hox-A1⁻/hox-A1⁻* animals

Hox-A1⁻/hox-A1⁻ animals have previously been observed to retain Vth ganglia and peripheral nerves, which appear normal with respect to their size and position (Lufkin et al., 1991; Chisaka et al., 1992). This is supported by the current observations because no major differences were apparent in the size of the ganglion, the position of the cranial nerve, the initial central projections of afferent fibers, or the placement and size of the trigeminal motor pools between the control and mutant animals. Fig. 3 illustrates a comparison between the appearance and position of the branchiomotor pools in control heterozygote versus mutant mice. For this comparison, 18 E11.5 embryos were injected with DiI only in the Vth ganglion. DiI provides a stronger fluorescence emission than DiO under the available excitation conditions, resulting in brighter labeling of the trigeminal branchiomotor neurons than was available in the double-labeled preparations. These embryos showed no major differences in the positioning of the trigeminal motor neurons between control and mutant animals. In these cases, neurons were present both anteriorly and posteriorly to the nerve entry point. By comparison

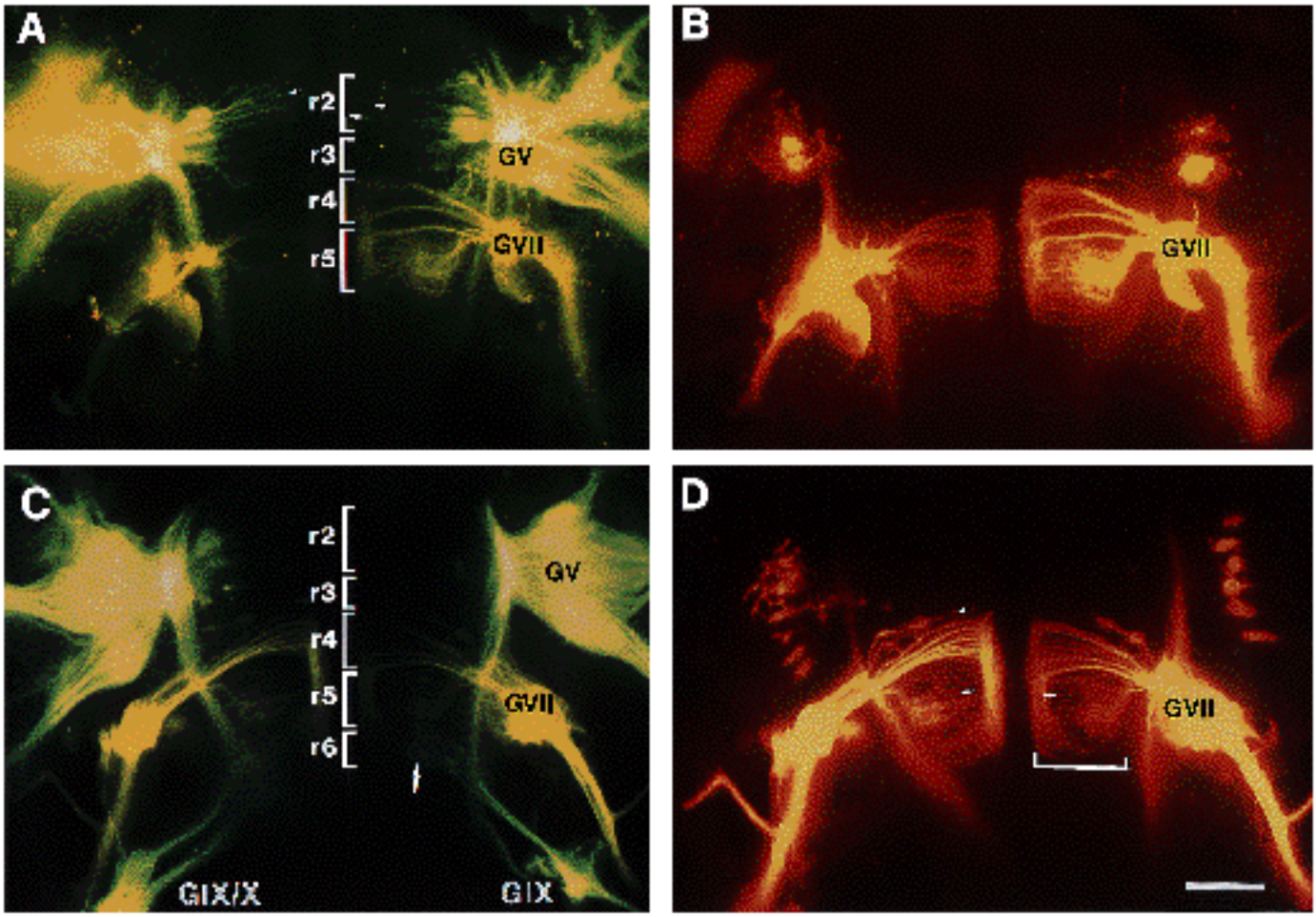

Fig. 2. Bilateral views of the ventral surface of hindbrain and associated cranial ganglia in E11.5 *hox-A1*$^{+}$*/hox-A1*$^{-}$ control mouse embryos. A, B and C, D are paired views of the same hindbrains using a fluorescein filter set (A,C) and a rhodamine filter set (B,D). In both pairs of figures, the Vth ganglia (GV) were injected with DiO and the VIIth/VIIIth ganglia (GVII) were injected with DiI. In C and D, the IXth and Xth ganglia (GIX, GIX/X) were also injected with DiO. In A and C, using the fluorescein filter set, both DiO (green) and DiI-labeled (yellow-green) structures are visible. In B and D, the DiI-labeled (red) VIIth/VIIIth ganglia, nerves, and efferent neurons are visible. DiO injection sites into the Vth ganglia, but no DiO-labeled structures, are also visible in B and D; because of the high concentration of DiO at these sites, there is some bleed-through at the rhodamine excitation wavelength. Branchiomotor neurons of the Vth cranial nerve, labeled with DiO, are visible in rhombomeres (r) 2 and 3 (A - brackets). A few of these neurons are indicated with small white arrows in A. Neurons of the VIIth/VIIIth nerve, labeled with DiI, are visible in r4 and r5 (B,D). Small white arrows in D indicate a few of these neurons. Neurons of the IXth nerve, labeled with DiO, are visible in r6 (C - arrow). Note that the cell bodies and efferent nerve fibers contributing to cranial nerves VII and VIII form a fan-shaped structure on each side of the hindbrain (B,D). The bracket in D indicates the mediolateral extent of the fan.In all plates, the midline and floorplate run down the center of the plate (visible in B and D) and anterior is up. Scale bar, 400 μm.

with double-labeled material (Figs 2, 4) and by comparison with published chick data (Lumsden and Keynes, 1989), this would place these neurons in rhombomeres 1, 2, and 3. Neurons are located as far medially as the lateral edge of the floorplate (visible as a dark band down the right side of Fig. 3A) in both mutants and controls. One slight difference between mutants and controls was the trajectory followed by the most posterior neurons in rhombomere 3 as they exited the hindbrain. Neurons at this location in control animals made a sharp anterior turn to exit the hindbrain, while similarly positioned neurons in mutant animals made a slightly shallower turn (Fig. 3). This may reflect some changes in the organization of rhombomere 3 that will be further elucidated below. However, the organization and position of trigeminal branchiomotor neurons was sufficiently similar between mutant and control as to suggest that there were no major changes in this region of the hindbrain. For these reasons, we used the position of the Vth cranial nerve and its associated motor pools as fixed landmarks by which to judge the differences in position of the other cranial nerves and efferent neurons in mutant animals.

Previous studies detected an anterior shift of the developing otocysts and of the VIIth/VIIIth and IXth cranial ganglia in *hox-A1*$^{-}$*/hox-A1*$^{-}$ embryos towards the trigeminal ganglion (Chisaka et al., 1992). This shift was often asymmetric, with the otocyst and associated ganglia on one side

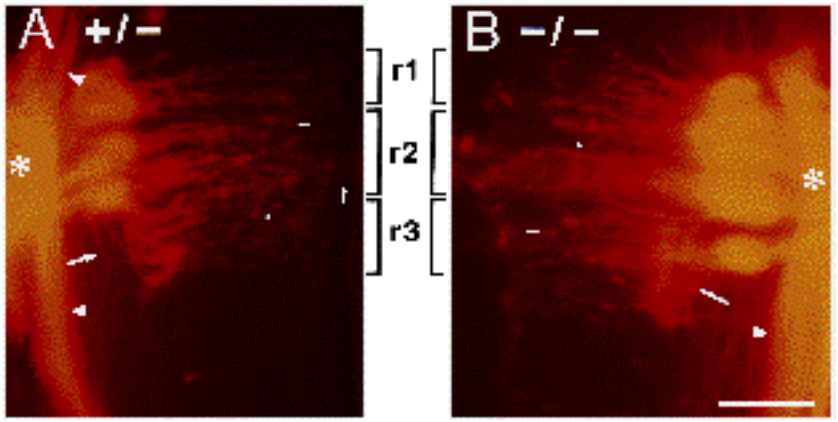

Fig. 3. Ventral view of the right side of the hindbrain in a *hox-A1*$^{+}$/*hox-A1*$^{-}$ (A) and the left side of the hindbrain in a *hox-A1*$^{-}$/*hox-A1*$^{-}$ (B) embryo. In both embryos, DiI was injected into the Vth cranial ganglion. Labeled afferent fibers enter the lateral edge of the hindbrain (asterisks in A and B) and bifurcate into ascending and descending branches in the ventrolateral mantle region (arrowheads). In both embryos labeled efferent neurons (small arrows)are visible in rhombomeres (r) 1, 2, and 3 (brackets), and labeled neurons are present as far medially as the lateral edge of the floorplate. The floorplate is clearly visible on the right side of A (f); it is in the same medial position in B. Light scatter from small DiI crystals on the surface of the hindbrain in B is present over the floorplate in rhombomere 2; these are not labeled cells. Efferent fibers from neurons in the posterior part of rhombomere 3 make a sharp turn to enter the Vth nerve in control mice (A -arrow) and a shallower turn in mutant embryos (B - arrow). Scale bar, 100 μm.

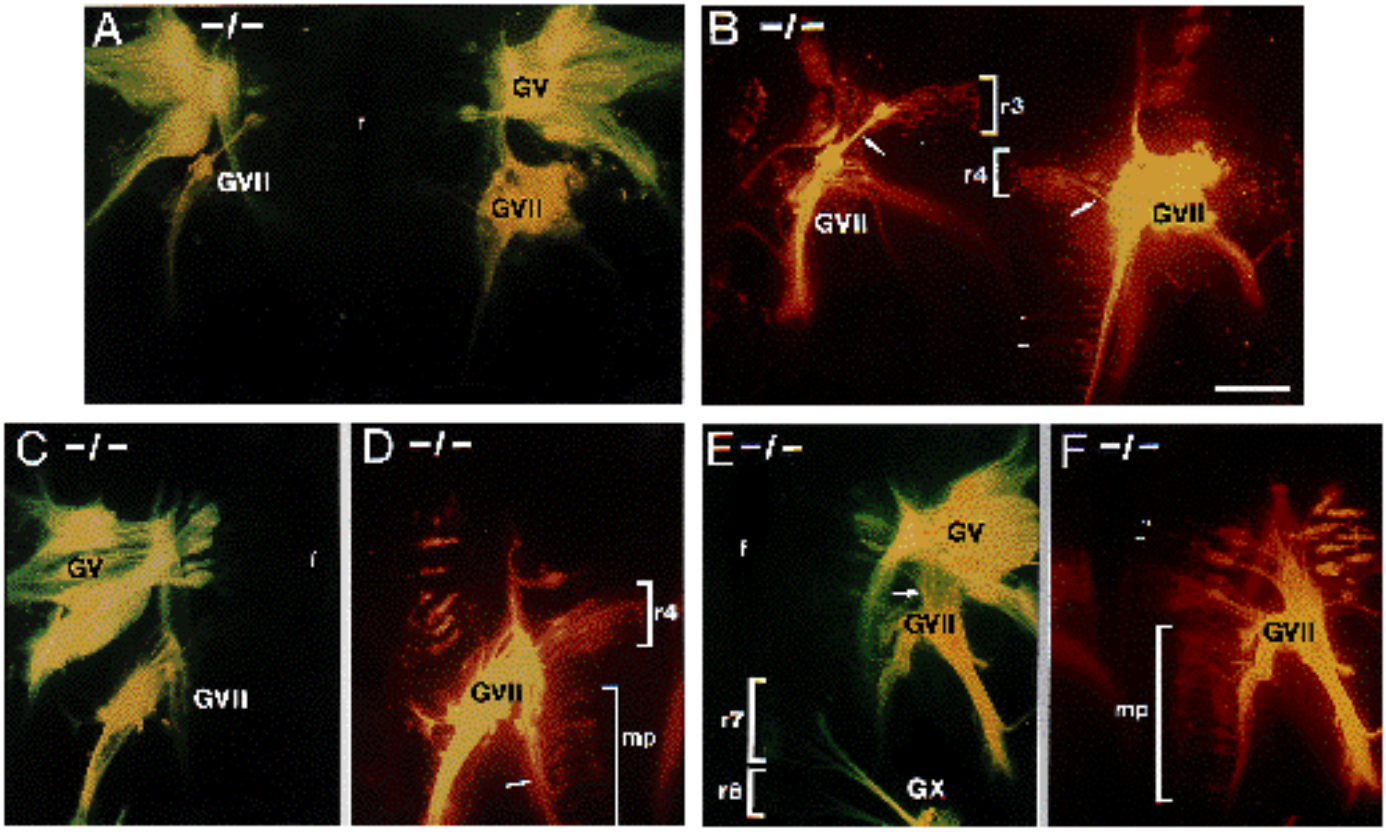

Fig. 4. Ventral surface of the hindbrain and associated cranial ganglia in three E11.5 *hox-A1*$^{-}$/*hox-A1*$^{-}$ mutant mouse embryos dissected and labeled as in Fig. 2. A and B, C and D, and E and F are paired views of the three hindbrains using a fluorescein filter set (A,C,E) and a rhodamine filter set (B,D,F). DiO and DiI are visible under different filter sets as described in the legend of Fig. 2. In all embryos, GV and GVII/VIII were injected with DiO and DiI, respectively. In E and F, GX was also injected with DiO. (A,B) Bilateral view of a mutant hindbrain. In B, some of the neurons projecting into the VIIth and VIIIth nerves are located in rhombomere (r) 3 on the left and r4 on the right (brackets). Additional neurons are positioned posteriorly within the hindbrain (small white arrows). The major trunk of the VIIth/VIIIth nerve is located more anteriorly on the left side of the figure than on the right (arrows). In A and B, the floorplate (f) is in the center of the plate and anterior is up. (C,D) Right side of a mutant hindbrain. In D, a large cluster of VIIth and VIIIth nerve neurons is positioned in r4 (bracket). Ectopic, DiI-filled neurons (mp) are also positioned at more posterior hindbrain levels, but project anteriorly (arrow) to join cranial nerve VII/VIII. The floorplate (f) is to the right and anterior is up. (E,F) Left side of the hindbrain in a mutant animal**.** The VIIth/VIIIth nerve is superimposed on GV (arrow in E). GX branchiomotor neurons are positioned medially in r7 and r8 (brackets in E). In F, ectopic DiI-filled neurons (mp) are positioned at posterior hindbrain levels, lateral to the position of GX motor neurons. Some neurons are also positioned anteriorly at the same level as the GV efferents (small arrows).The floorplate (f) is to the left and anterior is up. Scale bar, 400 μm.

positioned more anteriorly than the contralateral one (Chisaka et al., 1992). Injections of DiI into the VIIth/VIIIth cranial ganglia or nerves of *hox-A1*$^-$ homozygotes also demonstrated an anterior and asymmetric shift of these ganglia. The VIIth and VIIIth nerves sometimes entered the hindbrain at an apparently normal position (adjacent to rhombomere 4). However, in many mutant animals, the site of entry was shifted anteriorly, sometimes as far as rhombomere 2, resulting in the Vth and VIIth/VIIIth nerves entering the hindbrain at the same position (Fig. 4). In control animals, the VIIth/VIIIth nerve appeared as a single, tightly bound fascicle, whereas in the mutants, the main nerve was joined by multiple rootlets emerging from more posterior levels of the hindbrain (see below).

Dye fills of cranial neurons providing efferent fibers to cranial nerves VII and VIII showed that the positioning of these neurons was often also asymmetric across the midline, suggesting that the peripheral asymmetry was reflected in the organization of the hindbrain as well. In the mutant illustrated in Fig. 4A,B, the position of the VIIth and VIIIth efferent neurons on the left side of the figure is shifted to the same level as the contralateral Vth nerve, suggesting that the VIIth and VIIIth nerve efferent somata are positioned in rhombomere 3 instead of rhombomeres 4 and 5 (Fig. 4B, brackets). Conversely, the VIIth/VIIIth nerve efferents on the right side are positioned at the level of rhombomere 4 (Fig. 4B). The main neuron pools providing efferent fibers to cranial nerves VII and VIII on both sides appear to be restricted to an anterior-posterior span approximately the length of a single rhombomere. Axons traveling to cranial nerves VII and VIII in *hox-A1*$^-$*/hox-A1*$^-$ embryos were never observed to form the characteristic fan shape seen in rhombomeres 4 and 5 of control embryos (compare Figs 2 and 4). Instead, in most cases, the largest population of VIIth/VIIIth nerve neurons was positioned adjacent to the nerve entry point in what was sometimes rhombomere 4 and sometimes a more anterior rhombomere (Fig. 4C,D). In normal animals, more laterally positioned motor neuron cell bodies contributing fibers to cranial nerve VII would be found in rhombomere 5 (see Fig. 2). In *hox-A1*$^-$*/hox-A1*$^-$ embryos, laterally positioned cell bodies were not seen in the expected area. Often, there was a gap posterior to the main cluster of neurons where no labeled neurons were seen (Fig. 4D). Instead, there were populations of neurons positioned far posteriorly in the hindbrain that also contributed fibers to the VIIth/VIIIth cranial nerve (designated mp in Fig. 4D,F). These neurons are in the region of the hindbrain that would normally provide motor innervation to the IXth and Xth cranial nerves, but are located laterally to the position that would be occupied by the IXth and Xth nerve motor neurons. Fig. 4E,F illustrates a mutant embryo in which the VIIth/VIIIth ganglion was filled with DiI and the Xth ganglion was filled with DiO. In this embryo, the Xth ganglion motor pools were positioned more medially than the posterior neurons. Axons from these aberrantly positioned neurons travelled anteriorly from their point of origin and exited the brain near the entry point of the VIIth/VIIIth nerve, often contributing to the more posterior nerve rootlets that fuse with the VIIth/VIIIth nerve lateral to the hindbrain as described above (Fig. 4).

The IXth and Xth cranial ganglia were injected with DiO in 5 of the 18 mutant animals examined. Previous observations of *hox-A1* mutant mice have illustrated that the IXth and Xth ganglia are shifted anteriorly similar to the shift seen of the VIIth/VIIIth ganglion, again concurrently with a forward shift of the otocyst (Chisaka et al., 1992). The data presented here confirm the earlier observations. In four out of the five mutant embryos, the IXth ganglion did not make connections with the hindbrain. In these cases, no afferent fibers were observed emerging from the ganglion and travelling toward the hindbrain. In the exceptional case, the IXth nerve did connect with the hindbrain, but its entry point was shifted anteriorly with respect to its normal position in relation to the Vth cranial nerve. In this case, the motor pool providing efferent fibers to this nerve was also shifted anteriorly (data not shown). The Xth nerve makes connections with the hindbrain in most mutant animals; in cases where the Xth ganglion was clearly labeled with DiO, the positioning of motor neurons appears normal in relation to the midline of the animal (Fig. 4E).

Expression of *krox-20* is altered in *hox-A1*$^-$*/hox-A1*$^-$ mice

Our observations following dye injections into the cranial ganglia of *hox-A1*$^-$ mutant mice suggested that there are severe defects in the developing hindbrain, possibly including the absence of rhombomere 5. To address this possibility, we examined the expression patterns of 3 different genes, *krox-20*, *int-2* (*fgf-3*) and *hox-B1*, which are expressed in rhombomere 5 and/or in its neighboring rhombomeres during hindbrain development.

Krox-20, a gene encoding a zinc-finger protein, is transiently expressed in the hindbrain at the level of rhombomeres 3 and 5 (Wilkinson et al., 1989a). In early embryos (E8, 0-2 somite pairs) *krox-20* is expressed as a single band at the level of presumptive rhombomere 3. This initial expression precedes the formation of morphological rhombomere boundaries. This is followed at E8.5 (7-8 somite pairs) by expression in two bands at the levels of rhombomeres 3 and 5. By E9.5 *krox-20* expression is observed in only a single band in the hindbrain in rhombomere 5.

Using in situ hybridization to whole mouse embryos, the *krox-20* expression pattern was compared in *hox-A1*$^-$*/hox-A1*$^-$ mice to that in littermate controls. As expected, control embryos with 7-8 somite pairs expressed *krox-20* in two bands corresponding to the levels of rhombomeres 3 and 5 (Fig. 5, upper). In *hox-A1*$^-$*/hox-A1*$^-$ embryos at the same stage (i.e. having the same number of somite pairs), *krox-20* expression was seen in only a single band (Fig. 5, lower). In mutant animals this band is wider and exhibits less intense *krox-20* expression than in controls. Based on its position relative to the telencephalon, the heart and the first somite, as well as its temporal profile, this band of expression is at the level of rhombomere 3. Expression of this band in mutant embryos commences at E8.0, continues through E8.5 and recedes by E9.0 concurrent with the timing of *krox-20* expression in rhombomere 3 of control animals. We have never observed even a remnant of *krox-20* RNA expression at the level of rhombomere 5 in E8.5 mutant embryos or at later stages of embryogenesis. Thus, at E9.5 when control embryos clearly show only a single band of *krox-20* expression in rhombomere 5, no *krox-20* expression was

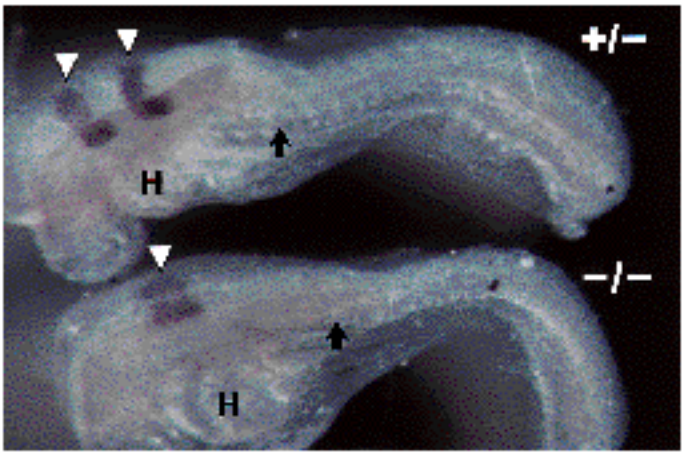

Fig. 5. Expression of the *krox-20* gene in the hindbrain of E8.5 mouse embryos. Shown are lateral views of whole mounts of 7 somite *hox-A1*$^{+}$*/hox-A1*$^{-}$ (upper) and *hox-A1*$^{-}$*/hox-A1*$^{-}$ (lower) littermates hybridized with a digoxigenin-labeled *krox-20* antisense RNA probe. Note the two stripes of *krox-20* expression in r3 and r5 in the heterozygote (arrowheads), and the single stripe at the level of r3 in the homozygote (arrowhead), consistent with the absence of r5 in the *hox-A1*$^{-}$*/hox-A1*$^{-}$ embryo. The arrow indicates the position of the first somite. H, heart. Scale bar, 150 μm.

detected by RNA in situ hybridization to sectioned *hox-A1*$^{-}$ homozygous mutant embryos (data not shown). Examination of dorsal and lateral views of *krox-20* expression in intact E8.5 mutant embryos also suggests that there is a shortening in the caudal region of the hindbrain, because the distance between the anterior limit of *krox-20* expression in rhombomere 3 and the first somite is approximately 20% shorter in mutant animals than in controls (Fig. 5). These observations are consistent with the suggestion that at least rhombomere 5 is missing in *hox-A1*$^{-}$*/hox-A1*$^{-}$ embryos.

int-2^{lacZ} expression in *hox-A1*$^{-}$ homozygotes

At E9.5, *int-2 (fgf-3)* is normally expressed in hindbrain rhombomeres 5 and 6, which are adjacent to the otocysts (Wilkinson et al., 1988). In order to follow *int-2* expression during the development of *hox-A1* mutants, we used mice in which the *E. coli lacZ* reporter gene was targeted into the *int-2* locus (Mansour et al., 1990; Mansour et al., 1993). Mice heterozygous for this allele (*int-2*$^{+}$*/int-2*^{lacZ}) appear normal, and the expression pattern of the *lacZ* reporter gene accurately reflects the known *int-2* RNA expression pattern (Wilkinson et al., 1988; Mansour et al., 1993). Fig. 6A shows a control E9.5 embryo (*hox-A1*$^{+}$*/hox-A1*$^{-}$, *int-2*$^{+}$*/int-2*^{lacZ}) reacted with X-gal. β-galactosidase activity was observed in the hindbrain adjacent to the otocyst and spanning the width of the otocyst. In *hox-A1*$^{-}$ homozygotes, the anteroposterior length of blue stained cells appears to be only half as wide as in the control, approximately the length of a single rhombomere (Fig. 6B). Eleven *hox-A1*$^{-}$*/hox-A1*$^{-}$, *int-2*$^{+}$*/int-2*^{lacZ} embryos were examined and this restriction of β-galactosidase activity to a single rhombomere was observed in all cases.

Coronal sections through the hindbrain of these animals further illustrate the confinement of *int-2* expression to a single rhombomere in the mutant embryos. β-galactosidase expression in control animals, visualized by dark-field optics as a pink reaction product, is in rhombomeres 5 and 6 (Fig. 6C). In mutant animals, β-galactosidase expression is greatly reduced and confined to a much smaller anterior-posterior region of the hindbrain, approximately equivalent to the length of one rhombomere (Fig. 6D). In the postulated absence of rhombomere 5, this *int-2* expression would be in rhombomere 6. β-galactosidase expression remains adjacent to the otocyst, though the otocyst is shifted anteriorly, often farther on one side of the animal than the other. This suggests that rhombomere 6 may also be shifted anteriorly. The reduction of *int-2* expression in the hindbrain of *hox-A1*$^{-}$*/hox-A1*$^{-}$ mice is specific to this site, as other regions of *int-2* expression do not appear to be affected in *hox-A1*$^{-}$ homozygotes, either qualitatively or quantitatively (data not shown). This may reflect the activity of *hox-A1* in regulating the expression of *int-2*, either directly or indirectly, or in a reduction in the number of *int-2*-expressing cells within this rhombomere.

Expression of *hox-B1* in *hox-A1*$^{-}$ homozygotes

At E9.5, *hox-B1* is normally expressed in the hindbrain in rhombomere 4 (Wilkinson et al., 1989b; Frohman et al., 1990; Murphy and Hill, 1991). Fig. 7B shows this expected expression of *hox-B1* in a coronal section through the hindbrain of a control *hox-A1*$^{+}$*/hox-A1*$^{-}$, E9.5 embryo. The anterior and posterior boundaries of *hox-B1* expression are sharp, and the posterior boundary of expression is at the level of the anterior margin of the otocyst. In a mutant embryo, the level of *hox-B1* expression in rhombomere 4 is reduced, the anteroposterior length of this rhombomere is shortened, and the relative position of *hox-B1* expression has changed such that the posterior boundary is now at the level of the anterior one-third of the otocyst (Fig. 7E).The borders of the domain of expression, particularly the posterior border, are less well defined relative to control animals and there appear to be patches of cells that do not express *hox-B1* dispersed among *hox-B1*-expressing cells. This is particularly evident in views of rhombomere 4 at higher magnification (Fig. 7C,F). In control animals the distribution of autoradiographic grains reflecting *hox-B1* RNA appears uniform over the entire rhombomere, but in *hox-A1*$^{-}$*/hox-A1*$^{-}$ mice, large patches of cells that do not express *hox-B1* were observed.

DISCUSSION

Cranial development in vertebrate embryos has been proposed to rely upon hindbrain segmentation, with the identity of structures arising at different levels of the head specified by their positional relationship with the developing brain (reviewed by Hunt et al., 1991). Therefore, alterations in hindbrain segmentation could affect the formation of adjacent head structures. Previous observations have shown that targeted disruption of the murine homeobox gene *hox-A1* results in developmental defects in the ear, cranial nerves and hindbrain (Lufkin et al., 1991; Chisaka et al., 1992). These defects are restricted to a defined region in the

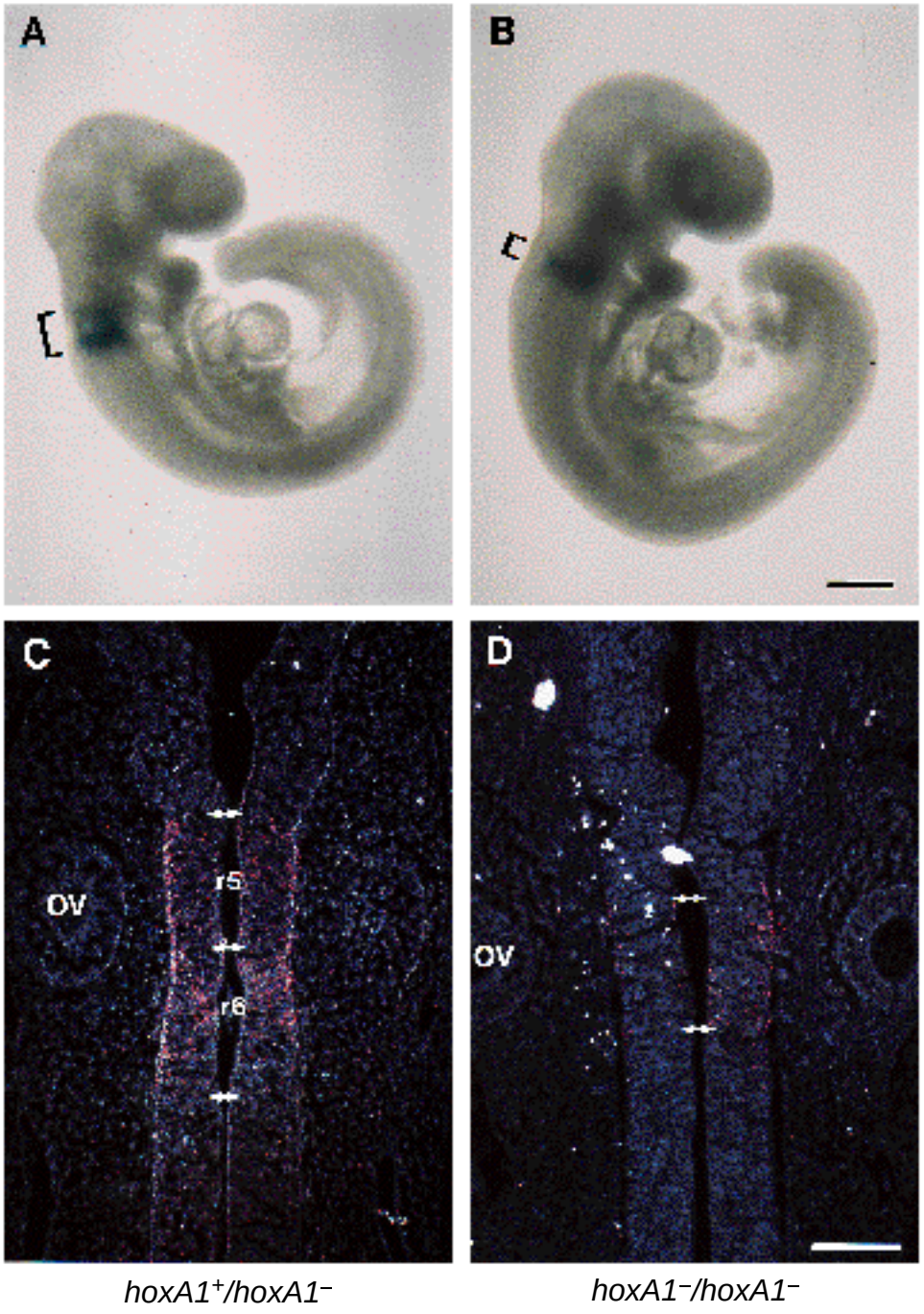

Fig. 6. Expression of *int-2*^{lacZ} in the hindbrain of E9.5 heterozygous control and *hox-A1*$^{-}$ homozygous embryos. (A,B) Staining of whole embryos for β-galactosidase activity using X-Gal. Note that the A-P length of the resulting blue stain in the *hox-A1*$^{+}$*/hox-A1*$^{-}$ control embryo (A) is approximately twice that of the *hox-A1*$^{-}$*/hox-A1*$^{-}$ embryo (B). Scale bar, 500 μm. (C,D) Coronal sections of embryos stained as above. In dark-field, the blue stain resulting from β-galactosidase activity appears pink. The double arrows indicate the extent of *int-2*^{lacZ} expression in r5 and r6 of the control embryo (C) and in approximately one rhombomere's length in the *hox-A1*$^{-}$*/hox-A1*$^{-}$ embryo (D). The embryos in A,B,C and D have 23, 24, 25 and 27 somite pairs, respectively. OV, otocyst. Scale bar, 100 μm.

head of the embryo adjacent to and including the hindbrain, with structures positioned anteriorly and posteriorly to this region apparently unaffected by the gene disruption. These defects may result from the action of *hox-A1* after appropriate formation of hindbrain segmentation or may result from a disruption of hindbrain segmentation itself.

The experiments we have described here provide a direct analysis of the cellular and molecular reorganization of the mouse hindbrain in the absence of the *hox-A1* gene. Our current observations suggest that hindbrain formation is severely affected in the mutant animals. First, there is a radical rearrangement of the branchiomotor neurons contributing to cranial nerve VII. Second, one stripe of *krox-20* expression, corresponding to the position of rhombomere 5, is absent, and the distance between the remaining stripe and the first somite is reduced. Third, *int-2* expression in the hindbrain is reduced from the normal expression observed in rhombomeres 5 and 6 to the approximate anteroposterior length of a single rhombomere. Fourth, the domain of expression of *hox-B1*, which normally marks rhombomere 4, is also reduced. Finally, the position of the domains of expression of *krox-20*, *int-2* and *hox-B1* in the *hox-A1*$^{-}$ homozygous embryos, relative to the positions of the otocyst, the trigeminal ganglion and the first somite, suggests a shortening of the posterior portion of the hindbrain. These results are schematically summarized in Fig. 8. The simplest inter-

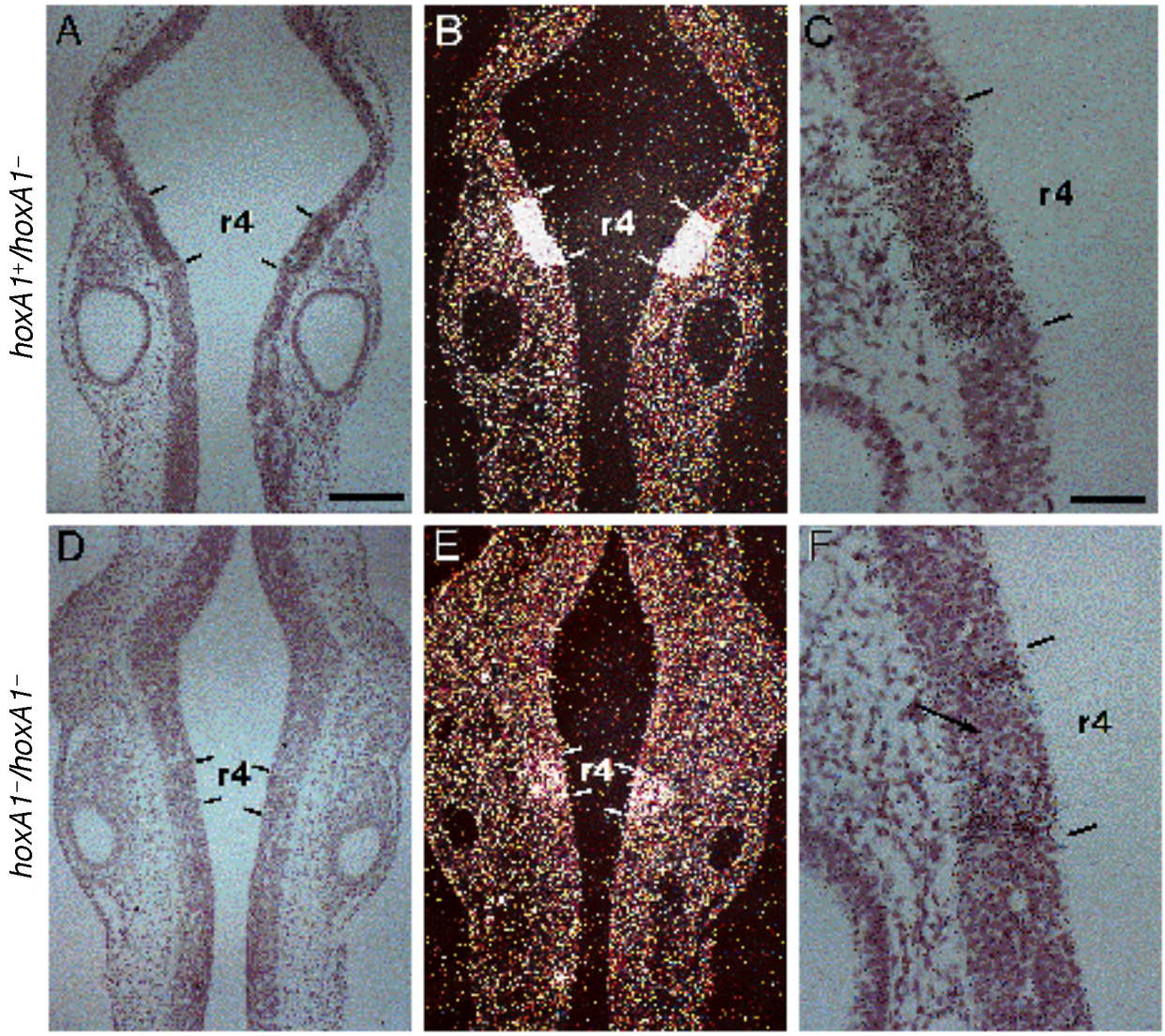

Fig. 7. *Hox-B1* expression in E9.5 heterozygous control and *hox-A1*⁻ homozygous mutant embryos. ^{35}S-labelled *hox-B1* antisense RNA probes were hybridized to 8 μm coronal sections of *hox-A1*$^{+}$/*hox-A1*⁻ (A-C) and *hox-A1*⁻/*hox-A1*⁻ (D-F) embryos. A,B and D,E are paired bright-field/dark-field views of the same section, while C and F are higher magnification views of different sections. The position of rhombomere (r) 4 is indicated in all panels. Rhombomere 4 appears smaller in mutant embryos (D,E) and shows a reduced level of *hox-B1* expression (compare B and E), with less precise posterior expression boundaries. In addition, the otocysts in the mutant (D,E) are smaller and laterally displaced compared with the heterozygous control (A,B), resulting in alteration of the relative position of *hox-B1*-expressing cells with respect to the otocyst. In F, patches of cells that do not express *hox-B1* (arrow) are interspersed with labeled cells. Scale bars, A, 170 μm; C, 50 μm.

pretation of our data suggests that the absence of *krox-20* expression in rhombomere 5, the reduction of the extent of *int-2* expression from two rhombomeres to one, the loss of the rhombomere 5 lateral motor nuclei that normally would send efferent fibers to the VIIth nerve, and the shortening of the hindbrain are a consequence of the physical absence of at least rhombomere 5. Alternatively, there could be a compression in this region of the hindbrain with a concomitant respecification of the cells in rhombomere 5, such that the morphological and molecular markers that normally characterize this rhombomere are no longer valid.

It should be emphasized, however, that the changes in the hindbrain of *hox-A1*⁻/*hox-A1*⁻ mice extend well beyond defects in rhombomere 5. The patterns of expression of *krox-20*, *hox-B1*, and *int-2*, as well as the position and projections of hindbrain efferent neurons, all suggest that the loss of *hox-A1* affects regions of the hindbrain from rhombomere 3 to rhombomere 8. The expression pattern of *hox-B1* argues that rhombomere 4 is affected. *Hox-B1* expression is reduced in *hox-A1*⁻ homozygotes, the boundaries of its domain are ill-defined, and patches of cells that do not express *hox-B1* often are interspersed among the *hox-B1*-expressing cells. This may reflect the absence of a well-defined border between rhombomere 4 and its posteriorly adjacent rhombomere. Rhombomere transplantation experiments have suggested that when rhombomeres 4 and 6 are positioned adjacent to

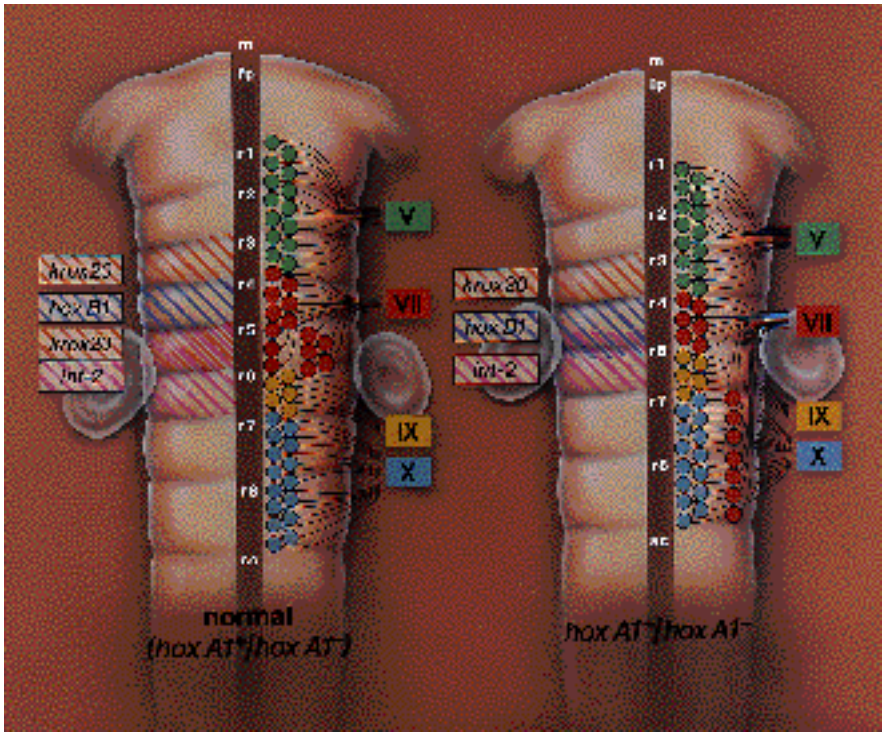

Fig. 8. Schematic representation of *krox-20*, *hox-B1*, and *int-2* expression and of neuronal organization in hindbrains of control (*hox-A1*$^{+}$*/hox-A1*$^{-}$) and mutant (*hox-A1*$^{-}$*/hox-A1*$^{-}$) mice. In control mice, *krox-20* is expressed in rhombomeres (r) 3 and 5 (yellow stripes), *hox-B1* is expressed in r4 (blue stripes), and *int-2* is expressed in r5 and r6 (pink stripes). In mutant mice, in the postulated absence of r5, *krox-20* is expressed in r3, *hox-B1* is expressed in r4, and *int-2* is expressed in r6. There may be mixing of cells between rhombomeres 4 and 6, indicated by the overlap of the domains of *hox-B1* and *int-2* expression. Neuronal organization in control mice is illustrated in Fig. 1 and is reiterated here for comparison with mutant mice. In the mutant mice we propose that the remaining VIIth/VIIIth efferent neurons are restricted to r4, with additional ectopic neurons positioned laterally in r7 and r8 (red circles). IXth (yellow circles) and Xth (blue circles) nerve motor neurons are positioned in the appropriate rhombomeres (r6 - IX, r7 and r8 - X), which are shifted anteriorly in the absence of r5. In most *hox-A1*$^{-}$ homozygotes, however, connections between the IXth ganglion and a motor pool in the displaced 6th rhombomere are not observed. Morphologic boundaries between adjacent rhombomeres are drawn for clarity in the *hox-A1*$^{-}$*/hox-A1*$^{-}$ schematic, but are missing in the mutant animals examined. Additionally, the otocyst, illustrated adjacent to r5 and r6 in normal animals, is shifted anteriorly and often asymmetrically in mutant animals.

each other, cells from these two rhombomeres may intermix (Guthrie and Lumsden, 1991). In the absence of rhombomere 5 in *hox-A1*$^{-}$*/hox-A1*$^{-}$ animals, cells from rhombomeres 4 and 6 would be positioned adjacent to each other and might be expected to intermix. This might explain why *hox-B1*-expressing cells, possibly derived from rhombomere 4, are intermingled with cells that do not express *hox-B1*, possibly derived from rhombomere 6. Alternatively, the presence of cells that do and do not express *hox-B1* in rhombomere 4 may reflect a requirement for *hox-A1* function to maintain *hox-B1* expression in a subset of cells in rhombomere 4. As a further example of possible cell mixing across rhombomere boundaries, the borders of *int-2* expression in the *hox-A1*$^{-}$ homozygous mice are less well defined than those of normal control mice and patches of cells that do and do not express *int-2* are interspersed to a greater extent in mutant embryos than in controls (see Fig. 6D). Dye-labeled cells expected to arise from rhombomere 4 are positioned sometimes at the appropriate level and sometimes more anteriorly, suggesting some variability in the degree to which rhombomere 4 is affected. The observation that efferents of the VIIth/VIIIth cranial nerve are often found in rhombomere 3 suggests that this rhombomere also is affected by the *hox-A1*$^{-}$ mutation, as does the observation that the band of *krox-20* expression in this rhombomere is wider and less intense than in control embryos. Finally, the observation that a new population of lateral motor nuclei that send efferent fibers to cranial nerve VII are present in rhombomeres 6, 7 and 8, suggests that these three rhombomeres are also abnormal in *hox-A1*$^{-}$*/hox-A1*$^{-}$ mice.

The interpretation of the perturbed pattern of hindbrain efferent neurons in the *hox-A1*$^{-}$*/hox-A1*$^{-}$ mice is complex, but is consistent with the observed changes in gene expression. In agreement with the interpretation that at least rhombomere 5 is missing, is the observed loss of the highly organized fan-shaped projections of efferent fibers to cranial nerve VII/VIII. This fan is generated by fibers emanating from sensory efferent and branchiomotor nuclei present in rhombomeres 4 and 5. In the mutant mice, the major nucleus associated with the VIIth/VIIIth cranial nerve is often restricted to an area the size of a single rhombomere and the more lateral motor neuron pool, normally present in rhombomere 5, is not observed. The remaining cluster of VIIth/VIIIth nerve neurons is sometimes positioned posterior to the level of the trigeminal nerve, at what would normally be the level of rhombomere 4, or can be positioned more anteriorly, overlapping the trigeminal motor domain at the level of rhombomere 3. Two explanations may be offered for this finding. In the absence of *hox-A1* function, the boundary between rhombomeres 3 and 4 may be altered so that neurons generated in rhombomere 4 may be able to migrate into rhombomere 3 and vice versa. Alternatively, the motor neurons positioned in rhombomere 3 which project into the VIIth/VIIIth nerve may have arisen in rhombomere 3 and, due to the close proximity of an anteriorly shifted VIIth nerve in mutant animals, sent their axons into that nerve. Areas of the hindbrain anterior to rhombomere 3 are apparently unaffected by the *hox-A1* mutation, as the trigeminal branchiomotor system is virtually unchanged in the mutant animals. *Hox-A1* has been shown by in situ

hybridization to be expressed to an anterior limit between rhombomeres 3 and 4 (Murphy and Hill, 1991), also suggesting that more anterior regions of the hindbrain are not likely to be directly affected by changes in *hox-A1* expression.

In mutant embryos, cranial nerves VII and VIII also receive efferent fibers from neurons that are positioned at more posterior levels of the hindbrain. These neuronal cell bodies are situated more laterally than the normal IXth and Xth nerve motor neuron pools and send axons laterally and anteriorly to exit the hindbrain either at the level of the VIIth and VIIIth cranial nerve, or as a series of smaller rootlets posterior to the entry point of this nerve. The behavior of these neurons is reminiscent of some of the motor neurons normally situated in rhombomere 5, which are also positioned laterally and which project axons laterally and then anteriorly to exit the brain at rhombomere 4. These presumptive ectopic VIIth nerve motor neurons may have two possible origins. They may be motor neurons that arose in an anterior rhombomere but because of weakened rhombomere boundaries, were able to cross into more posterior hindbrain levels. Alternately, these cells might have arisen in more posterior rhombomeres, but had their fate respecified in the absence of the *hox-A1* gene.

The dramatic reorganization of the hindbrain, affecting the robustness of multiple rhombomeres, suggests a general role for *hox-A1* in controlling the proliferation of cells within the developing hindbrain. A reduction in cell proliferation would explain the shortening of the caudal hindbrain. However, this is not a general effect on the entire hindbrain because some rhombomeres are affected more than others. Whereas rhombomeres 4 and 6 may be reduced in size, rhombomere 5 appears to be missing. Changes in the formation of the rhombomeres could subsequently lead to the observed disorganization of the branchiomotor neuron system, including the changes in the efferent and afferent projection patterns, the loss of some motor neurons, as well as the presence of ectopic motor neurons.

The observed hindbrain reorganization may also offer an explanation for the previously reported displacement of the otocyst and cranial nerves VII/VIII, IX and X towards the trigeminal ganglion. The precursor to the otocyst, the otic placode, forms in the surface ectoderm adjacent to the hindbrain (Altman and Bayer, 1982). The otic vesicle invaginates from this placode to form the otocyst. Neural crest cells contributing to the VIIth cranial ganglion congregate anterior to the otocyst while cells contributing to the IXth and Xth ganglia coalesce posterior to the otocyst (Altman and Bayer, 1982). Embryo transplantation experiments have suggested that the formation and position of the otocyst may depend on signal(s) emanating from the hindbrain (for review see Noden and Van De Water, 1986). The variable extent of the anterior shift of the VIIth and VIIIth efferent neurons could be accompanied by a parallel change in the position of the source for the otocyst-inducing signal, which in turn would reposition the otocyst and associated ganglia.

Hox-A1^{-}/*hox-A1*$^{-}$ mice are also afflicted with major defects in the formation of the inner ear (Lufkin et al., 1991; Chisaka et al., 1992). Continued development of the otocyst to a functional ear is dependent on *int-2* expression (Mansour et al., 1993). Decreased levels of *int-2* expression in *hox-A1*$^{-}$/*hox-A1*$^{-}$ embryos, caused partly by the absence of one of the rhombomeres where it is normally expressed and partly through down regulation of its expression in rhombomere 6, would compromise continued development of the otocyst into a functional inner ear. This down regulation may reflect activity of *hox-A1* in the regulatory pathway for *int-2*. Whether there is a direct or indirect interaction between *int-2* and *hox-A1* is not known.

In conclusion, examination of the hindbrain of *hox-A1*$^{-}$/*hox-A1*$^{-}$ mice using a variety of markers suggests radical rearrangments in its formation. The effects of the *hox-A1* mutation extend from rhombomere 3 through rhombomere 8, but appear to be essential for the formation of rhombomere 5. The appearance of ectopic neurons in rhombomere 6, 7 and 8 also suggests a role for *hox-A1* in the specification of cell identity and/or cell migration in the hindbrain. Previously, by analogy to the function of genes in the Homeotic Complex of *Drosophila*, it has been suggested that the mammalian *Hox* genes might be involved in the specification of cells within rhombomeres, but not in the formation of the segmental units themselves. In *Drosophila*, one set of genes, including the *gap, pair-rule* and *segment polarity* genes, is used to establish the segmental pattern of the embryo. A different set of genes is used to specify the identity of each segmental unit (i.e. the *Hom-C* genes). The results herein suggest that in mammals the same set of genes, the *Hox* genes, may be used both to form the rhombomeres in the hindbrain and to specify the identity of cells within these segments. By controlling the proliferation of specific cells within a region of the developing embryo, the *Hox* genes could unite these two processes.

We thank B. Condie for providing the *krox-20* clone used for whole-mount in situ hybridization and J. McMahon for help with whole-mount in situ protocols. We are particularly grateful to Dr Drew Noden for sending us maps of the mouse branchiomotor pool prior to publication and for critically reading this manuscript. We also thank S. Tamowski, R. Hayes and B. Mickelsen for mouse husbandry, S. Mansour for help with dark-field photomicroscopy, and L. Oswald for help with the preparation of the manuscript.

REFERENCES

Altman, J. and Bayer, S. (1982). Development of the cranial nerve ganglia and related nuclei in the rat. In *Advances in Anatomy, Embryology and Cell Biology* vol. 74, pp. 1-90. New York: Springer-Verlag.

Bally-Cuif, L., Alvarado-Mallart, R.-M., Darnell, D. K. and Wassef, M. (1992). Relationship between *Wnt-1* and *En-2* expression domains during early development of normal and ectopic met-mesencephalon. *Development* **115,** 999-1009.

Chavrier, P., Zerial, M., Lemaire, P., Almendral, J., Bravo, R. and Charnay, P. (1988). A gene encoding a protein with zinc fingers is activated during G_0/G_1 transition in cultured cells. *EMBO J.* **7,** 29-35.

Chisaka, O., Musci, T. S. and Capecchi, M. R. (1992). Developmental defects of the ear, cranial nerves, and hindbrain resulting from targeted disruption of the mouse homeobox gene *Hox-1.6*. *Nature* **355,** 516-520.

Duboule, D. and Dollé, P. (1989). The structural and functional organization of the murine *Hox* gene family resembles that of *Drosophila* homeotic genes. *EMBO J.* **8,** 1497-1505.

Fraser, S., Keynes, R. and Lumsden, A. (1990). Segmentation in the chick embryo hindbrain is defined by cell lineage restrictions. *Nature* **344**, 431-435.

Frohman, M. A., Boyle, M. and Martin, G. R. (1990). Isolation of the mouse *Hox-2.9* gene; analysis of embryonic expression suggests that positional information along the anterior-posterior axis is specified by mesoderm. *Development* **110**, 589-607.

Graham, A., Papalopulu, N. and Krumlauf, R. (1989). The murine and *Drosophila* homeobox gene complexes have common features of organization and expression. *Cell* **57**, 367-378.

Guthrie, S. and Lumsden, A. (1991). Formation and regeneration of rhombomere boundaries in the developing chick hindbrain. *Development* **112**, 221-229.

Harland, R. M. (1991). In situ hybridization: an improved whole mount method for *Xenopus* embryos. *Meth. Cell Biol.* **36**, 685-695.

Hunt, P., Whiting, J., Nonchev, S., Sham, M., Marshall, H., Graham, A., Cook, M., Allemann, R., Rigby, P. W. J., Gulisano, M., Faiella, A., Boncinelli, E. and Krumlauf, R. (1991). The branchial Hox code and its implications for gene regulation, patterning of the nervous system and head evolution. *Development* **Supplement 2**, 63-77.

Lufkin, T., Dierich, A., LeMeur, M., Mark, M. and Chambon, P. (1991). Disruption of the *Hox-1.6* homeobox gene results in defects in a region corresponding to its rostral domain of expression. *Cell* **66**, 1105-1119.

Lumsden, A. (1990). The cellular basis of segmentation in the developing hindbrain. *Trends Neurosci.* **13**, 329-335.

Lumsden, A. and Keynes, R. (1989). Segmental patterns of neuronal development in the chick hindbrain. *Nature* **337**, 424-428.

Lumsden, A., Sprawson, N. and Graham, A. (1991). Segmental origin and migration of neural crest cells in the hindbrain region of the chick embryo. *Development* **113**, 1281-1291.

Mansour, S. L., Thomas, K. R., Deng, C. X. and Capecchi, M. R. (1990). Introduction of a *lac-Z* reporter gene into the mouse *int-2* locus by homologous recombination. *Proc. Natl. Acad. Sci. USA* **87**, 7688-7692.

Mansour, S. L., Goddard, J. M. and Capecchi, M. R. (1993). Mice homozygous for a targeted disruption of the proto-oncogene *int-2* have developmental defects in the tail and inner ear. *Development* **117**, 13-28.

Marshall, H., Nonchev, S., Sham, M. H., Muchamore, I., Lumsden, A. and Krumlauf, R. (1992) Retinoic acid alters hindbrain Hox code and induces transformation of rhombomeres 2/3 into a 4/5 identity. *Nature* **360**, 737-741.

McMahon, A. P. and Bradley, A. (1990). The *Wnt-1* (*int-1*) proto-oncogene is required for development of a large region of the mouse brain. *Cell* **62**, 1073-1085.

Murphy, P., Davidson, D. R. and Hill, R. E. (1989). Segment-specific expression of a homeobox-containing gene in the mouse hindbrain. *Nature* **341**, 156-159.

Murphy, P. and Hill, R. E. (1991). Expression of the mouse *labial*-like homeobox-containing genes, *Hox-2.9* and *Hox-1.6*, during segmentation of the hindbrain. *Development* **111**, 61-74.

Noden, D. M. and Van De Water, T. R. (1986). The developing ear: tissue origins and interactions. In *The Biology of Change in Otolaryngology*. (eds. R. J. Ruben, T. R. Van De Water, and E. W. Rubel), pp. 15-46. Amsterdam: Elsevier.

Scott, M. P. (1992). Vertebrate homeobox gene nomenclature. *Cell* **71**, 551-553.

Serbedzija, G. N., Bronner-Fraser, M. and Fraser, S. E. (1992). Vital dye analysis of cranial neural crest migration in the mouse embryo. *Development* **116**, 297-307.

Wilkinson, D. G., Peters, G., Dickson, C. and McMahon, A. P. (1988). Expression of the FGF-related proto-oncogene *int-2* during gastrulation and neurulation in the mouse. *EMBO J.* **7**, 691-695.

Wilkinson, D. G., Bhatt, S., Chavrier, P., Bravo, R. and Charnay, P. (1989a). Segment-specific expression of a zinc-finger gene in the developing nervous system of the mouse. *Nature* **337**, 461-464.

Wilkinson, D. G., Bhatt, S., Cook, M., Boncinelli, E. and Krumlauf, R. (1989b). Segmental expression of *Hox-2* homeobox-containing genes in the developing mouse hindbrain. *Nature* **341**, 405-409.

(Accepted 13 May 1993)